INNOSTORAGE – USE OF INNOVATIVE THERMAL ENERGY STORAGE FOR MARKED ENERGY SAVINGS AND SIGNIFICANT LOWERING CO_2 EMISSIONS

Beneficiaries:

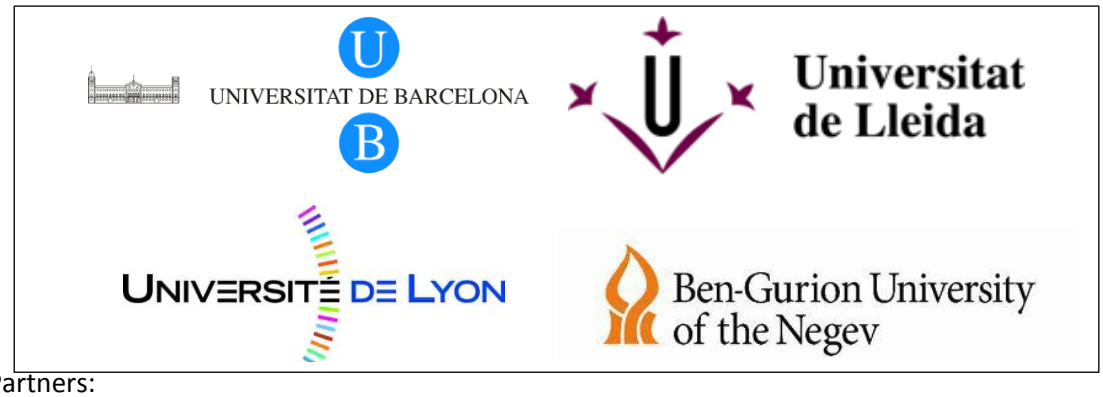

Partners:

D7.2 - Report on Staff Exchanges

	Name and Institution	Date
Prepared by:	Kévin Taurines Université de Lyon	18/12/2015
Checked by:		
Approved by:	Prof. Dr. Luisa F. Cabeza Universitat de Lleida	

Contents

1 Objectives 4

2 Introduction 5

3 Description of work 7

3.1 Ground model 8

3.2 Foundation model 12

3.3 PCM integration and modelling 13

4 Materials and Methodology 15

4.1 Spatial discretization 16

4.2 Temporal discretization 18

4.3 Boundary conditions 19

5 Results 21

6 Outcomes or future work 25

7 References 26

8 Assessment 28

Nomenclature

b_T, b_ψ	W.m^{-3}, s^{-1}	Boundary condition in heat and moisture transfer equations for ground model
b'_T, b'_P	W.m^{-3}, s^{-1}	Boundary condition in heat and moisture transfer equations for foundation model
B_T, B_Ψ		Boundary vector in set of heat and moisture transfer equations for ground model
B'_T, B'_P		Boundary vector in set of heat and moisture transfer equations for foundation model
C	J.m-^{3}K^{-1}	Bulk soil volumetric thermal capacity
c	J.kg^{-1}.K^{-1}	Specific heat
c_{TT}, c'_{TT}	J.m-^{3}K^{-1}	Thermal capacity in heat transfer equations for ground and for foundation model
$c_{T\Psi}, c'_{T\Psi}$	J.m^{-3}m	Hygric capacity in heat transfer equations for ground and for foundation model
$c_{\Psi T}, c_{PT}$	K^{-1}	Thermal capacity in moisture transfer equations for ground and for foundation model
$c_{\Psi\Psi}, c'_{PP}$	m^{-1}	Hygric capacity in moisture transfer equations for ground and for foundation model
C_{TT}		Thermal capacity matrix in set of heat transfer equations for ground model
$C_{T\Psi}$		Hygric capacity matrix in set of heat transfer equations for ground model
$C_{\Psi T}$		Thermal capacity matrix in set of moisture transfer equations for ground model
$C_{\Psi\Psi}$		Hygric capacity matrix in set of moisture transfer equations for ground model
D_{Tv}	m².s^{-1}.K^{-1}	Thermal vapour diffusivity
$D_{\Psi v}$	m.s^{-1}	Hydraulic vapour diffusivity
$\overrightarrow{g_T}$		Gravity (load) vector in heat transfer equations for ground model
$\overrightarrow{g_\Psi}$		Gravity (load) vector in moisture transfer equations for ground model
G_T		Gravity (load) vector in set of heat transfer equations for ground model
G_Ψ		Gravity (load) vector in set of moisture transfer equations for ground model
h_c	W.m^{-2}.K^{-1}	Convective exchange coefficient
k_{TT}, k'_{TT}	W.m^{-1}.K^{-1}	Thermal conductance in heat transfer equations for ground and for foundation model
$k_{T\Psi}, k'_{TP}$	J.m^{-3}.s^{-1}	Hygric conductance in heat transfer equations for ground and for foundation model
$k_{\Psi T}, k'_{PT}$	J.m^{-3}.K^{-1}	Thermal conductance in moisture transfer equations for ground and for foundation model
$k_{\Psi\Psi}, k'_{PP}$	m.s^{-1}	Hygric conductance in moisture transfer equations for ground and for foundation model
K_{TT}		Thermal conductance in set of heat transfer equations for ground model
$K_{T\Psi}$		Hygric conductance in set of heat transfer equations for ground model
$K_{\Psi T}$		Thermal conductance in set of moisture transfer equations for ground model
$K_{\Psi\Psi}$		Hygric conductance in set of moisture transfer equations for ground model
K_h	m.s^{-1}	Hydraulic conductivity
K_{rel}	-	Relative hydraulic conductivity
K_s	m.s^{-1}	Saturated hydraulic conductivity (m.s-1)
K_T	-	Thermal correction for hydraulic conductivity
L	J.kg^{-1}	Heat of vaporisation of water
n, m	-	van Genuchten exponents

m_l^t	kg	Quantity of liquid water on mesh I at t
P	Pa	Pressure
R	W.m^{-2}	Solar irradiation
R_v	J.kg^{-1}.K^{-1}	Vapour gas constant
S	-	Degree of saturation (-)
S_i	m²	Area of mesh i
T	K	Temperature
v	m.s^{-1}	Air velocity in the foundation
V	m.s^{-1}	Wind velocity
w	kg.m^{-3}	Total moisture content
W	kg_{vap}. kg_{as}^{-1}	Moisture content

Greek letters

α	m^{-1}	Van Genuchten shape factor
α_d	-	Soil dry surface albedo
γ	K^{-1}	Normalised thermal surface tension derivative
δ_v	S	Permeability for vapour pressure gradients
$\delta x, \delta y, \delta z$	m	Mesh size along x, y and z axis
Δt	s	Time step
ε	-	Ground surface emissivity
θ	m^3.m^{-3}	Volumetric content
λ	W.m^{-1}.K^{-1}	Thermal conductivity
ξ	-	Thermal gradient ratio in the concerned phase
ρ	kg.m^{-3}	Density
σ		Stefan-Boltzmann constant
Ψ	m	Matric head

Subscript

0	At reference temperature
a	Air
b, e, n, s, t, w	Bottom, East, North, South, Top and West interfaces
B, E, N, P, S, T, W	Bottom, East, North, current, South, Top and West nodes
c	Capilllary
l	Water - liquid
s	Solid - Saturation
S	Surface
v	Vapour
w	Cavity walls

1 Objectives

In the context of thermal comfort requirements of building occupants and the trend towards reduced energy consumption, passive technologies represent interesting solutions. Depending on the season, earth-to-air heat exchangers (EAHE) enable to preheat or cool air before inject it into the building, thanks to the thermal charge/discharge ground potential. Despite this, the uptake of building-integrated EAHE is somewhat limited, due typically to a lack of space in the building grounds, and the additional costs implied for the subterranean piping. This study considers therefore an innovating EAHE which is an element of the building envelope: a geothermal foundation (Figure 1).

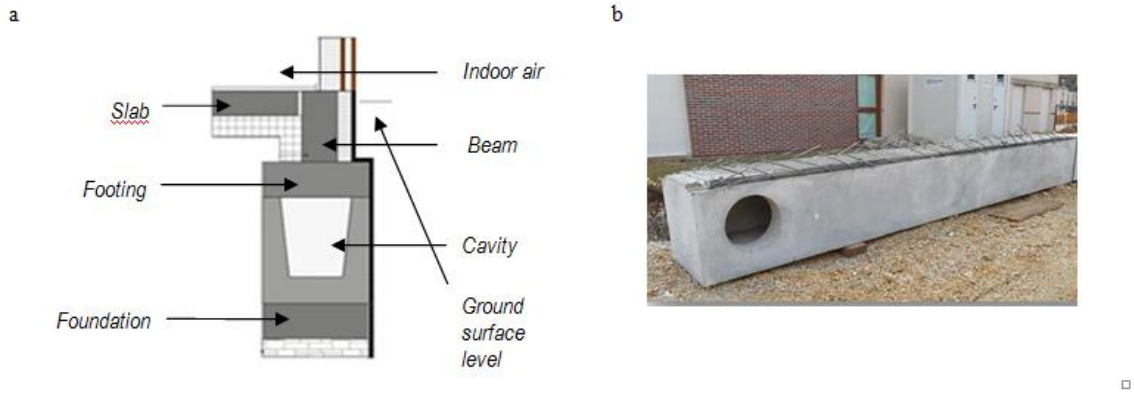

Figure 1 : Cross section of the foundation studied (a) and general view of the FONDATHERM product (b)

The concrete prefabricated hollowed foundation replaces a classical EAHE duct generally in PVC, tackling the problems previously cited. This foundation is called FONDATHERM according to the name of the project whose aim is to attain a better understanding of the behaviour of this system, and study innovating coupling with other energy systems (heat pump, solar chimney, PCM, etc.). EAHE have been widely studied in the past, but three mains features of FONDATHERM compared to classical EAHE motivate this study:

1) Firstly, the foundation is exposed simultaneously to climatic stresses on one side and to building conditions (via the beam and slab) on the other side. Classical EAHE are either buried below the building or more often lie far from the building, and are consequently exposed to only one kind of stress.
2) Secondly, FONDATHERM is usually buried at a depth of 50 cm to 1.5 m, shallower than traditional EAHE buried at a depth of about 2m. Thus, FONDATHERM is highly impacted by the weather which means that potential energy saving (heat gain or loss according to the season) can be less substantial. For this reason, an accurate modelling of the foundation seems to be necessary.
3) Finally, the duct is concrete which means that contrary to PVC pipe it will allow mass transfer that can obviously changed the thermal behaviour of the foundation.

In this context, our objectives during the secondment are first to develop a coupled heat and mass transfer model of the foundation and its vicinity ground. Secondly we want to study the opportunity to add PCM into the foundation in order to improve its functioning during mid season. The study will try to answer the following questions:

a) Is it possible to integrate PCM into the concrete of a foundation or on the cavity walls?
b) Under which conditions do these combined systems enable us to improve the performance of the foundation? Is it possible to reach daily phase shifting?

2 Introduction

As stated above, a lot of studies have been published about EAHE. In [1], the authors developed a coupled heat and mass transfer model of EAHE which is solved with TRNSYS. It takes into account 2D radial and axial heat and moisture transfer within the ground. The influence of ground surface is simply modeled by an undisturbed ground temperature, which assumes that ground thermal properties are homogeneous. This model is validated against experimental data obtained from a pipe buried 1.5m below the surface, but for data spanning only a short period of 13 summer days. Gauthier and al. [2] carried out a numerical study of an EAHE buried below a building based on a 3D finite difference model. This model enables to use non homogeneous ground properties, dynamic boundary conditions and sensible and latent transfer within the pipes. Moisture transfers into the ground are considered negligible by the authors. This model was validated thanks to experimental data, but again only for a short period of 3 days. Hollmuler developed during his PhD work [3] both an analytical model and a 3D finite element model of EAHE. As the analytical model was mainly used to give a better understanding of EAHE and to enable to size it, it's not flexible enough for complex geometry. For the numerical model, he made the same assumption as Gauthier et al. [2]: no mass transfer within the ground and heat and mass transfer between the circulating air and the pipes walls. His model is validated against experimental data spanning several months recording, but only on fully summer or winter period. Thiers and Peuportier [4] modelled the coupling between a double-flow air handling unit and an EAHE using COMFIE. The ground is modelled as a semi-infinite solid with constant and homogeneous thermal properties, and the presence of water is once again neglected. Tittelein and al. [5] proposed a new approach using the response factor method in order to reduce the computational time. The ground is divided into 2D vertical slices, and each slice is modelled by a response factor method with different factors. The response factors are obtained from a finite element model. The authors pointed out the limits of their model: axial heat transfer is neglected and ground surface boundary condition model doesn't enable to take into account shadow or complex solicitations. Trząski and Zawada [6], developed a quasi 3D transient model based on finite element method, but only sensible heat transfers are taken into account. The moisture presence is modeled by a seasonal corrective factor of the thermal conductivity. The authors of [7] used a linear 2D cylindrical model to study a deep buried EAHE. The ground surface influence is thus considered as negligible and a ground undisturbed model is used to compute the temperature of the

boundary layer of the ground around the pipe. In [8] the authors chose to solve the Navier-Stokes equations to describe air temperature and velocity within the pipe, which are solved using Fluent. Ground water content is not taken into account, and ground surface boundary conditions are simplified by the use of undisturbed ground temperature. They compared their model to experimental results got from a 2m depth EHAE: the relative difference between measures and model are between 4 and 16%. In [9], Bansal and al. also used a CFD model to compute the air domain. The model was developed within the GAMBIT software. The same kind of assumptions has been made: constant and homogeneous ground thermal properties, undisturbed ground temperature far away from the pipe. The difference between experimental data on a 3.7m depth EHAE and modeling are under 8%. In both cases, measures are one-off, and only on short periods (less than 2 days).

In his recent study, Gan [10] give a summary of all the limits of the kind of model previously cited: the thermo-physical properties of the ground is highly dependent on the moisture content and humidity of ground can strongly vary in shallow ground. He stresses the need to use 3D model, to take into account interactions between the pipe and the soil but also between the pipe and the atmosphere. He use a full 3D coupled heat and mass transfer model. Furthermore, [11], [12], [13] and [14] clearly show the importance of ground water content on building heat loss via the ground. All these elements comfort us in the idea that the model to describe the behavior of the foundation has to be 3D, to take into account heat and mass transfers, and allow accurate evaluation of heat and mass transfer at the ground surface.

In the same way, phases change materials (PCM) are also good solution to save energy provided that their sizing is adapted. They have been embedded into various building construction materials successfully in the past. In [15], the authors carried on an experimental study consisting in integrate micro-encapsulated PCM in plaster board (made by Dupont de Nemours) and in evaluate the dampening of the thermal wave due to the adding of these sheets. A model based on an equivalent specific heat is used to evaluate the heat flow with and without PCM. The authors of [16] studied numerically and experimentally brick filled with paraffin and use an enthalpy method to develop their own model.

Other authors studied coupling or integration of PCM with air handling units or ventilated elements integrated into building envelope. A numerical and experimental study of a latent heat thermal energy storage combining PCM and heat exchanger has been carried on in [17]. The PCM model is based on an enthalpy formulation. This TES is used to supply fresh air to individual houses. A numerical study of a ventilated facade which embeds PCM using an equivalent specific heat method has been investigated in [18]. In [19] the authors proposed a new kind of TES, consisting in a hollowed ceiling panel in which outdoor air can circulate before to be injected into the building. Both experimental and numerical studied are lead. A 3D model using the equivalent specific heat capacity method for the gypsum layer and a 1D model for the air flow are used.

This brief literature review clearly shows that first there is a lack of knowledge about the behaviour of EAHE during the mid season. In our specific case where the foundation is not buried deeply, its operating is highly influence by climate. The energy savings could be sparse or inexistent. The first experimental results got from the FONDATHERM project confirm this fact, as shown on Figure 2. When the air temperature is higher than the ground mean temperature, the air is cooled when it goes through the foundation. This is obviously not desirable: the objective is to warm it up as long as its temperature does not reach the thermal comfort level. These kinds of inefficient periods have to be investigated and forecast in order to mitigate them, or at least to know when ventilation of the foundation should be avoided.

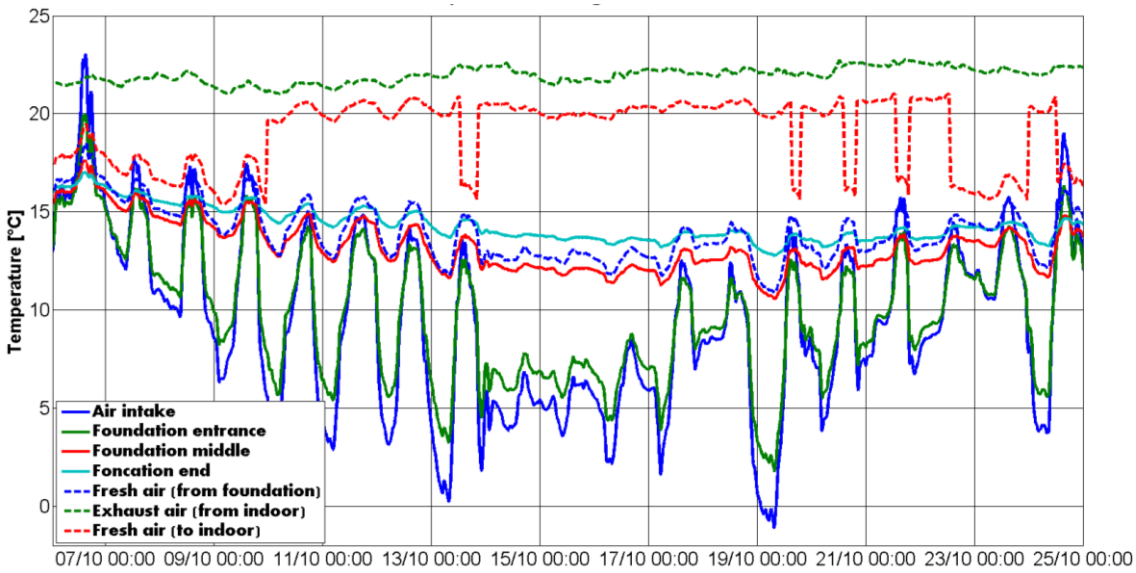

Figure 2 : Air temperature along the foundation (experimental results)

Secondly, it appears that such study requires using an accurate 3D model, taking into account simultaneous heat and mass transfer within the ground and the concrete foundation. Boundary conditions have to be described as accurately as possible.

Finally, using a coupling between PCM and EAHE could be a solution to avoid the period when EAHE operates intermittently. It's indeed possible to dampen and shift the thermal outdoor wave though the introduction of PCM. This has already been proved by studies of the behaviour of building construction material or air handling units incorporating PCM. But as far as we know, only a few papers about coupling between PCM and EAHE can be found in literature. Rodrigues and Gillot [20] studied experimentally a coupling between an EAHE and PCM embodied in wallboards. This system seems to be very promising even though a good regulation is needed.

3 Description of work

In our case, the idea is to develop a system as simple as possible, which can be connected to every kind of air handling units. Thus, we are going to study the foundation coupled with

PCM embodied in its walls. Our objective is to evaluate the relevance of this system, and investigate the energy saving and thermal performance of the foundation.

3.1 Ground model

First, we are going to develop an accurate ground model, which has to be flexible enough to model different kind of grounds, geometry and boundary conditions, and which allow us to make a coupling with a foundation and a PCM model. Nonetheless, we have to keep in mind that we usually have very few information about the soil nature on a full scale experiment. Consequently, a trade-off has to be made between very accurate model and high number of parameters involved.

A lot of papers have been published on heat and mass transfer in porous media. Almost all the formulations used nowadays are widely inspired by the work of Philip and De Vries [21], [22]. Nevertheless, the appropriate approach to writing this equation and to compute the parameters remains a subject of active discussion. The mains changes or discussion are on:

a) The choice of the variable to describe the water content of the ground. Several choices can be made at this stage: the water content θ $(m^3.m^{-3})$, the capillary pressure p_c (Pa), the vapour density ρ_v $(kg.m^{-3})$, or the matric head Ψ (m). In order to model the ground, which is a specific case of porous media, the matric head seems to be the most relevant choice. It enables to model saturated media as well as saturated media which is not the case of p_c and ρ_v. Furthermore, this variable is continuous even when there is a change in ground material, which is not the case with θ.

b) The way to compute the ground thermal conductivity. The form proposed by (De Vries, [23] (Equation (1)) is widely accepted [12], [13], but there are some divergences about the way to compute the parameters ξ_i $(-)$, [24] the thermal gradient in the phase i.

$$k = \frac{\theta_l \lambda_l + \xi_p \theta_p \lambda_p + \sum_{s=1}^{n} \xi_s \theta_s \lambda_s}{\theta_l + \xi_p \theta_p + \sum_{i=1}^{n} \xi_s \theta_s} \quad (1)$$

c) The water retention curve, i.e. the link between the water content θ and the matric head Ψ. Once again, several models exist, the one proposed in [25] and (Equation (2)) has been shown to give really good results for a large range of soils, and used in a lot of further work [26]. Some authors like Mualem [27] and Janssen [13] chose to include a hysteresis model into this retention curve.

$$\theta = \theta_r + (\theta_s - \theta_r)(1 - (-\alpha\Psi)^n)^{-m} \quad (2)$$

d) The ground hydraulic conductivity. Using the models proposed by [25], [26], [28], and [29], Janssen [13] proposed a new model (Equation (3)).

$$K_h = K_s K_{rel} K_T \quad (3)$$

where $K_{rel} = S^{\tau}\left(\frac{1-(1-S^{1/m})^{m}}{1-(1-S0^{1/m})^{m}}\right)^{2}$ $(-)$is the correction factor to take into account the saturation degree of the ground, and $K_T = 1.12\ 10^{-4}T^2 - 4.12\ 10^{-2}T + 3.46\ (-)$ is a viscosity dependent temperature correction

All the physical quantities discussed above and developed in [13] offer the great advantages of being accurate whilst depending only on a limited number of parameters. A set of parameters for 7 kinds of soils got from statistics fitting with experimental data and representative of most of the traditional soils has been given in his work. In addition, the formulation of the heat and mass transfer equation he used is one of the most accepted in the field. For all these reasons we decided to adopt a similar system of equation for the ground. The resulting equations are given by Equation (4).

$$\begin{aligned} c_{TT}\frac{\partial T}{\partial t} + c_{T\Psi}\frac{\partial \Psi}{\partial t} - \nabla\cdot\left(k_{TT}\vec{\nabla}\mathrm{T} + k_{T\Psi}\vec{\nabla}\Psi + \overrightarrow{\mathrm{g_T}}\right) = b_T \\ c_{\Psi T}\frac{\partial T}{\partial t} + c_{\Psi\Psi}\frac{\partial \Psi}{\partial t} - \nabla\cdot\left(k_{\Psi T}\vec{\nabla}\mathrm{T} + k_{\Psi\Psi}\vec{\nabla}\Psi + \overrightarrow{\mathrm{g_\Psi}}\right) = b_\psi \end{aligned} \quad (4)$$

where

$$c_{TT} = C + \theta_a\left(L_0 + c_v(T-T_0)\right)\frac{\partial \rho_v}{\partial T} + \left(c_l\rho_l(T-T_0) - \rho_l W - c_v\rho_v(T-T_0) - \rho_v L_0\right)\frac{\partial \theta}{\partial T}$$

$$c_{T\Psi} = \theta_a\left(L_0 + c_v(T-T_0)\right)\frac{\partial \rho_v}{\partial \Psi} + \left(c_l\rho_l(T-T_0) - \rho_l W - c_v\rho_v(T-T_0) - \rho_v L_0\right)\frac{\partial \theta}{\partial \Psi}$$

$$c_{\Psi T} = \left(1-\frac{\rho_v}{\rho_l}\right)\frac{\partial \theta}{\partial T} + \frac{\theta_a}{\rho_l}\frac{\partial \rho_v}{\partial T}$$

$$c_{\Psi\Psi} = \left(1-\frac{\rho_v}{\rho_l}\right)\frac{\partial \theta}{\partial \Psi} + \frac{\theta_a}{\rho_l}\frac{\partial \rho_v}{\partial \Psi}$$

$$k_{TT} = \lambda_{eff} + c_l\rho_l(T-T_0)D_{Tv}$$

$$k_{T\Psi} = \rho_l L D_{\Psi v} + c_l\rho_l(T-T_0)(D_{\Psi v} + K_h)$$

$$k_{\Psi T} = D_{Tv}$$

$$k_{\Psi\Psi} = K_h + D_{\Psi v}$$

$\overrightarrow{\mathrm{g_T}} = \begin{bmatrix} 0 \\ 0 \\ c_l\rho_l(T-T_0)K_h \end{bmatrix}$, $\overrightarrow{\mathrm{g_\Psi}} = \begin{bmatrix} 0 \\ 0 \\ K_h \end{bmatrix}$ and B_T and B_ψ containing the boundary conditions

These equations take into account:

- Liquid transfer due to matric potential gradient i.e. suction (or pressure in case of saturation)
- Liquid transfer due to gravity

- Vapour transfers due to diffusion
- Vapour transfer due to temperature gradient
- Conductive heat transfer within the solid matric, the water and the moist air
- Advection heat transfer produce by liquid or vapour movement
- Latent heat transfer by evaporation and condensation between the water and the moist air filled pores.

These equations ignore:

- Air movement: air filled pores is supposed to be everywhere at atmospheric pressure
- Liquid transfer due to temperature gradient
- Contribution of water contained in the vapour phase on the total quantity of moisture.

Given the complexity of these equations, it seems important to check their accuracy. For this reason all the physical parameters used in the equations above have been compared against results got from [13] as shown in Figure 3, in order to be sure that the original equations are correct before discretisation. As said before, all these physical quantities have been computed using a set of parameters given by [13]. In the case below, the parameters have been set to model sand.

	This work	**(Janssen, 2002)**
$\boldsymbol{\lambda(\theta)}$	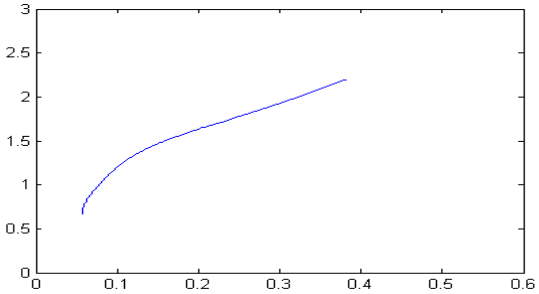	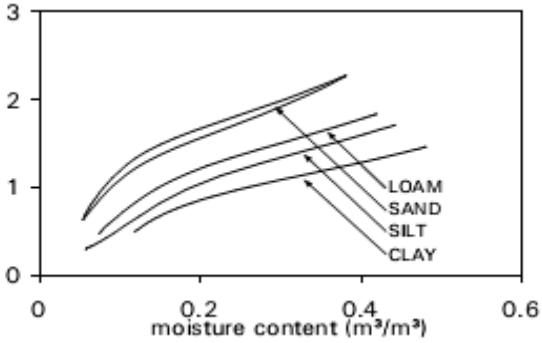
$\boldsymbol{D_{Tv}(\Psi)}$	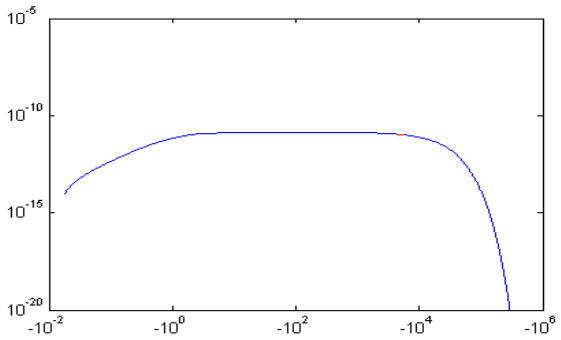	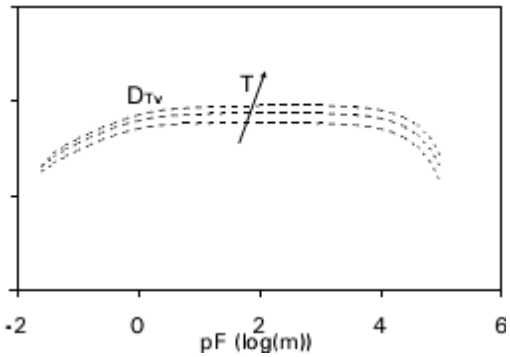

$D_{\Psi v}(\Psi)$

$K_h(\Psi)$

$C(\theta)$

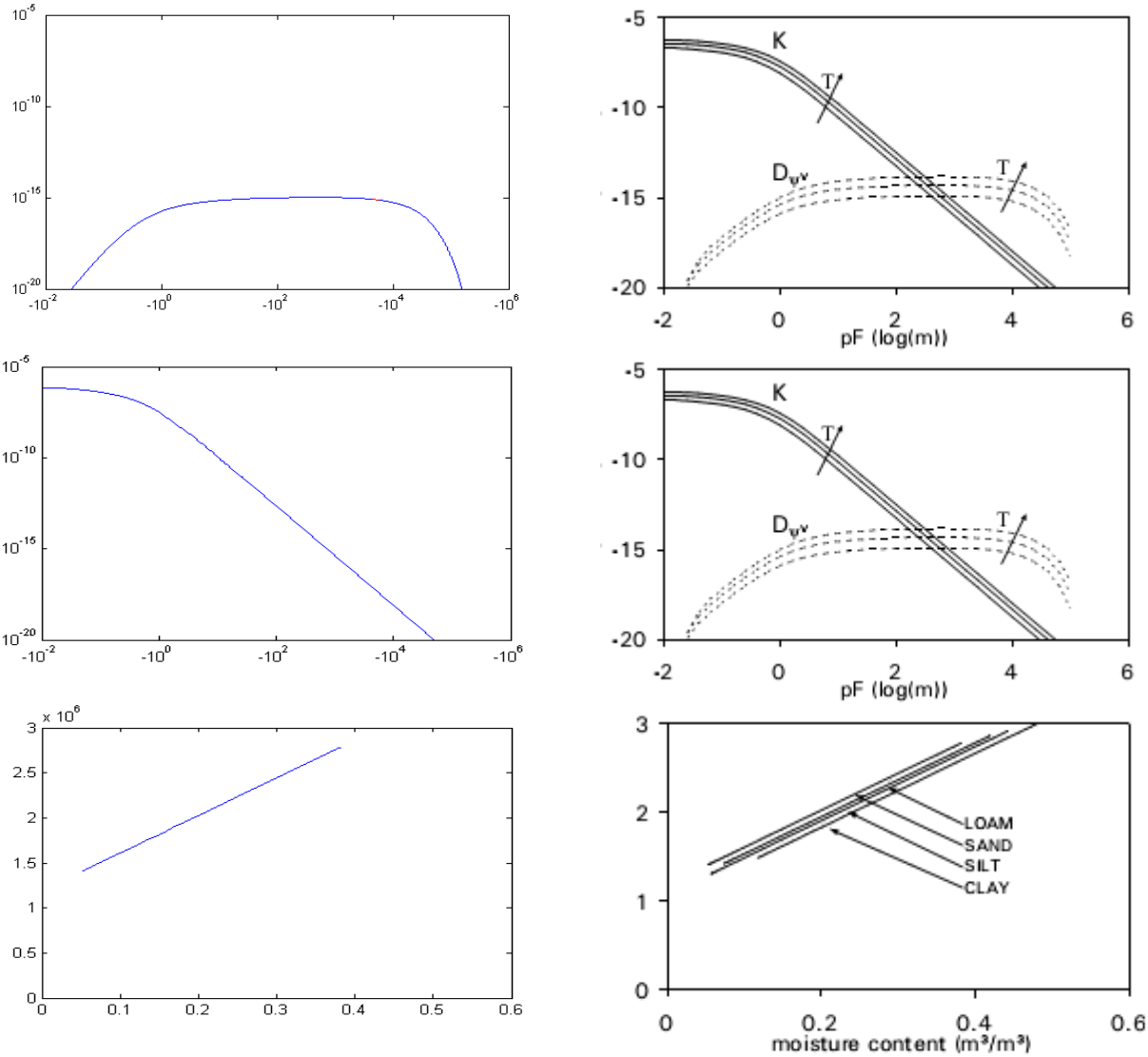

Figure 3 : Comparison between the main physical parameters used by Janssen and that which will be used in this work

3.2 Foundation model

The equations above are not adapted to model traditional building construction material like concrete or polystyrene. First because the formulation of all the parameters involved in the equations are specific to ground modeling. As the shape and the size of the pore can be completely different, it's impossible to find a set of parameters of the ground model that give the moisture retention curve, the hydraulic conductivity, etc. of the concrete for example. Building construction materials are also considered to be fully unsaturated. Using the matric head as the main variable to describe the state of the water is thus not appropriated.

Although some modifications are needed, the overall formulation of the equation to describe the foundation behavior is more or less the same. The same resolution method could be used for both the systems. (Berger [30] et Labat [31] proposes to use in his PhD work a system using the vapor pressure as potential. But the capillary pressure (the pressure difference between the liquid and gaseous phase in the pores) is usually preferred [32]. Furthermore, the link between the capillary pressure and the matric head is simple, given by the formula $P_c = \rho_l g \Psi$, which will enable us to easily construct the coupling between the ground model and the foundation model. For these reasons, we chose to use the capillary pressure based formulation, given by Equation (5).

$$\begin{aligned} c'_{TT}\frac{\partial T}{\partial t} + c'_{TP}\frac{\partial P_c}{\partial t} - \nabla\cdot\left(k'_{TT}\vec{\nabla}T + k'_{TP}\vec{\nabla}P_c\right) &= b'_T \\ c'_{PT}\frac{\partial T}{\partial t} + c'_{PP}\frac{\partial P_c}{\partial t} - \nabla\cdot\left(k'_{PT}\vec{\nabla}T + k'_{PP}\vec{\nabla}P_c\right) &= b'_P \end{aligned} \tag{5}$$

with

$$c'_{TT} = c_s\rho_s + c_l w$$

$$c'_{TP} = c_l T\frac{\partial w}{\partial P_c}$$

$$c'_{PT} = 0$$

$$c'_{PP} = \frac{\partial w}{\partial P_c}$$

$$k'_{TT} = \lambda + \frac{\delta_v P_v}{\rho_l R_v T^2}(c_v T + L_v)\left(\rho_l L_v + P_c(T\gamma - 1)\right)$$

$$k'_{TP} = c_l T K_h + \frac{\delta_v p_v}{\rho_l R_v T}(c_v T + L_v)$$

$$k'_{PT} = \frac{\delta_v P_v}{\rho_l R_v T^2}\left(\rho_l L_v + P_c(T\gamma - 1)\right)$$

$$k'_{\mathrm{PP}} = K_h + \frac{\delta_v p_v}{\rho_l R_v T}$$

Compared to the ground model, the dependence of water content w with temperature, the thermal vapour diffusion is neglected. The effect of gravity is also ignored. In [30] most of the needed parameters for some basic materials frequently used in buildings, among them the concrete, are available.

The coupling between the ground and the foundation model will be ensure via the temperature and the matric head at the interface, each one acting as a boundary condition for the two models. The whole model will be solved iteratively until convergence is achieved.

3.3 PCM integration and modelling

Several possibilities may be considered for the incorporation PCM into building elements. According to [33], we can distinguish:

- Direct incorporation which entails mixing PCM directly with construction materials such as gypsum or concrete. Although inexpensive, leakage problems may arise with this approach.
- The immersion approach, which involves immersing porous material (gypsum, brick, etc) into the melted PCM so that it is absorbed. This solution is also prone to leakage problems and possible interaction with building structure.
- Encapsulation (before incorporation) of the PCM, which can be divided in two types: micro and macroencapsulation. The containment may solve the leakage problem, protect the PCM, and should enhance the heat transfer with its environment.

Microencapsulation seems to be the most promising means to incorporate PCM, and has thus been chosen to add the function of energy storage into the foundation. Two construction techniques appear possible: the PCM can be incorporated into the concrete while the foundation is prefabricated, or alternatively sheets of microencapsulated PCM can be added to the cavity walls. The first solution may prove more difficult in practice because it can affect the mechanical strength of the foundation, and also it implies a change to the manufacturing process. On the other side, laying Dupont sheets onto the cavity wall seems fairly straightforward thanks to the U shape of the foundation as can be seen in Figure 4.

Figure 4 : Fondatherm before incorporation to building : adding Dupont de Nemours sheet in red

Once the choice of the way to integrate the PCM into the foundation has been made, we have to model the PCM and the coupling with the foundation. Several methods have been developed in the past to model PCM. Lamberg and al. [34] developed a model for PCM more rigorous, solving the Navier-Stockes equations for the melted PCM. Convection between the solid and liquid phases is neglected. Both enthalpy and equivalent specific heat methods are used in the heat equation and compared. In both cases, the model can reproduce accurately enough the PCM melting and solidification, but the model using equivalent heat specific method gives better results. The work in [35] is motivated by the fact that only a few models enable to model buildings integrating PCM, with reasonable time step without compromise the accuracy of the results on several years of simulation. Thus they compared 3 different models (enthalpy, equivalent specific heat and heat source) and 4 different schemes to solve the enthalpy model. Only a tridiagonal matrix algorithm with an iterative scheme and enthalpy formulation satisfy the conditions cited before. The authors of [36] also compared the equivalent specific heat model, the enthalpy model based on pure substance assumption and the enthalpy method based on binary mixture assumption. The results show that the latter model is the only one which can reproduce correctly the behaviour of the material. For the above reasons, there appear to be some divergences regarding the best way to model microencapsulated PCM. Finally the equivalent specific heat method has been chosen to model our system.

In addition, the PCM sheet that has to be laid onto the cavity wall is supposed to be fully impermeable. Thus, only one equation will be used to model this element, given by Equation (7).

$$\rho_{PCM} C_{PCM}(T) \frac{\partial T}{\partial t} = \nabla \cdot \left(\lambda_{PCM} \vec{\nabla} \mathrm{T}\right) \quad (6)$$

We supposed that both heat and mass transfer occur between the cavity walls and the circulating air. The Hollmuller method [3] which has been validated on experimental data is thus preferred, instead of the method exposed in [19] which doesn't take into account the mass transfers. The Hollmuller method is based on the Lewis assumption and is summarised

on Figure 5. The resulting equations are given by Equation (6). This equation has been implemented so that all the unphysical situations could be avoided:

- Each cavity wall mesh is independent: evaporation and condensation can happen simultaneously
- For condensation cases, the moisture exchange is set so that $W_{air,j}$ is not under 0. If $W_{air,j} < \frac{\sum_i S_i \frac{h_{c,i}}{c_a}(W_{air,j}-W_{w,ij})}{(c_a+c_v W_{a,j})\rho_{a,j} v}$, all the mass flow $S_i \frac{h_{c,i}}{c_a}(W_{air,j} - W_{w,ij})$ are multiply by a corrective factor $\frac{\left(\sum_i S_i \frac{h_{c,i}}{c_a}(W_{air,j}-W_{w,ij})\right)_{max}}{\left(\sum_i S_i \frac{h_{c,i}}{c_a}(W_{air,j}-W_{w,ij})\right)_{expected}}$
- For evaporation cases, the factor $\sum_i S_i \frac{h_{c,i}}{c_a}(W_{air,j} - W_{w,ij})$ can be unphysical for two reasons. First, the available water on the cavity wall may be not sufficient. Secondly because the circulating air reaches the saturation level before the quantity $\sum_i S_i \frac{h_{c,i}}{c_a}(W_{air,j} - W_{w,ij})$ has been evaporated. As for the condensation case, corrective factor have been implemented to avoid these unphysical situations.

$$T_{air,j+1} = T_{air,j} - \frac{\sum_i S_i h_{c,i}(T_{air,j} - T_{w,ij})}{(c_a + c_v W_{air,j})\rho_{a,j} v}$$

$$W_{air,j+1} = W_{air,j} - \frac{\sum_i S_i \frac{h_{c,i}}{c_a}(W_{air,j} - W_{w,ij})}{(c_a + c_v W_{a,j})\rho_{a,j} v} \quad (7)$$

$$m_l^{t+\Delta t} = m_l^t + \sum_i S_i \frac{h_{c,i}}{c_a}(W_{air,j} - W_{w,ij})$$

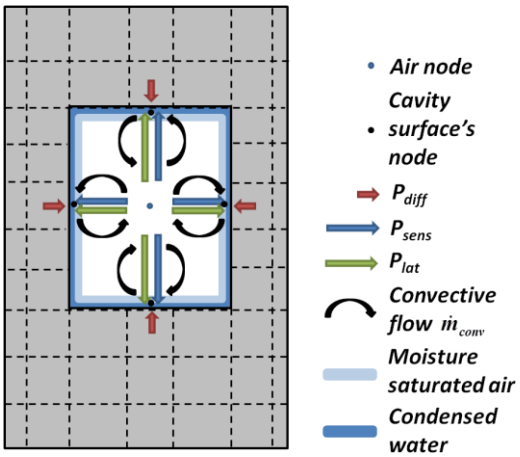

Figure 5 : Heat and mass transfer between the cavity walls of the foundation (or the PCM sheet) and the circulating air

4 Materials and Methodology

Once the modelling choices have been made, the physical equations have been implemented in a Matlab code. Given the complexity of the equations previously introduced, it's impossible to find an analytic (exact) solution. We can only approach the solution by a numerical estimation. The goal of the following treatment is thus to discretize spatially and temporally the equation (4) and (5), then to write a method to solve the resulting highly non linear equation.

4.1 Spatial discretization

Several methods of spatial discretization may be considered, the most famous ones are the finite element method, the finite volume method and the finite difference method. The finite element method is very stable, consistent but is quite hard to implement even for a Cartesian meshing. On the contrary the finite volume method is relatively easy to use with a simple meshing. In our case, where all the elements modelled are rectangular (except the foundation's cavity), we chose to use the last one method.

Finite volume method consists in integrate the continuous equations on a control volume. An example is given below for the ground heat equation, on a 3D meshing (a 2D example is given on fig by the sake of simplicity). Note that the choice has been made to set the node in the middle of each meshes, instead to set the interface in the middle of two nodes. Both have advantages and drawbacks according to Patankar [37], but the solution adopted was easier to code.

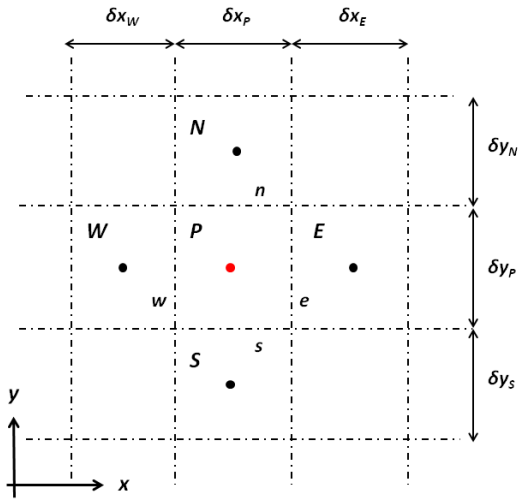

Figure 6 : 2D meshing for a finite volume method

Integration of heat equation on the control volume V_c around the node P, delimited by the surface Γ_c, forgetting at the moment the boundary conditions vector for the sake of simplicity and using the Green-Ostrogradski theorem, we have:

$$\iiint_{V_c} C_{TT}\frac{\partial T}{\partial t} + C_{T\Psi}\frac{\partial \Psi}{\partial t} = \iint_{\Gamma_c} (k_{TT}\nabla \mathrm{T} + k_{T\Psi}\nabla\Psi + \overrightarrow{g_T}) \cdot d\overrightarrow{\Gamma_c}$$

According [37], the first term of the right hand side of this equation (the second term gives a similar expression) become:

$$\iint_{\Gamma_c} (k_{TT}\vec{\nabla}\mathrm{T})\, d\overrightarrow{\Gamma_c} = (k_{TT}\vec{\nabla}\mathrm{T})_e \cdot \overrightarrow{\Gamma_e} - (k_{TT}\vec{\nabla}\mathrm{T})_w \cdot \overrightarrow{\Gamma_w} + (k_{TT}\vec{\nabla}\mathrm{T})_n \cdot \Gamma_n - (k_{TT}\vec{\nabla}\mathrm{T})_s \cdot \overrightarrow{\Gamma_s}$$
$$+ (k_{TT}\vec{\nabla}\mathrm{T})_t \cdot \overrightarrow{\Gamma_t} - (k_{TT}\vec{\nabla}\mathrm{T})_b \cdot \overrightarrow{\Gamma_b}$$

The evaluation of the coefficient k_{TT} on the interface e, w, n and s is done thanks to a geometric mean, and the evaluation of the temperature gradient is done by a central difference scheme which finally give us

$$\iint_{\Gamma_c} \left(k_{TT}\vec{\nabla}\mathrm{T}\right) d\overrightarrow{\Gamma_c} = \frac{2k_{TT_P}k_{TT_E}(T_E - T_P)}{k_{TT_E}\delta x_P + k_{TT_P}\delta x_E}\cdot \delta y_P \delta z_P - \frac{2k_{TT_W}k_{TT_P}(T_P - T_W)}{k_{TT_P}\delta x_W + k_{TT_W}\delta x_P}\cdot \delta y_{P\delta z_P}$$
$$+ \frac{2k_{TT_P}k_{TT_N}(T_N - T_P)}{k_{TT_N}\delta y_P + k_{TT_P}\delta y_N}\cdot \delta x_P \delta z_P - \frac{2k_{TT_S}k_{TT_P}(T_P - T_S)}{k_{TT_P}\delta y_S + k_{TT_S}\delta y_P}\cdot \delta x_P \delta z_P$$
$$+ \frac{2k_{TT_P}k_{TT_T}(T_T - T_P)}{k_{TT_T}\delta z_P + k_{TT_P}\delta z_T}\cdot \delta x_P \delta y_P - \frac{2k_{TT_B}k_{TT_P}(T_P - T_B)}{k_{TT_P}\delta z_B + k_{TT_B}\delta z_P}\cdot \delta x_P \delta y_P$$

As the vector $\overrightarrow{\mathrm{g_T}}$ has only a component along the z axis, we have

$$\iint_{\Gamma_c} \overrightarrow{\mathrm{g_T}}\cdot d\overrightarrow{\Gamma_c} = \left(\mathrm{g_{T,z,t}} - \mathrm{g_{T,z,b}}\right)\delta x_P \delta y_P$$

Using the same geometric mean assumption to compute $\mathrm{g_{T,z}}$ on the interfaces t and b, we get:

$$\iint_{\Gamma_c} \overrightarrow{\mathrm{g_T}}\cdot d\overrightarrow{\Gamma_c} = \mathrm{g_{T,P}}\left(\frac{\mathrm{g_{T,T}}(\delta z_P + \delta z_T)}{\mathrm{g_{T,P}}\delta z_T + \mathrm{g_{T,T}}\delta z_P} - \frac{\mathrm{g_{T,B}}(\delta z_P + \delta z_B)}{\mathrm{g_{T,P}}\delta z_B + \mathrm{g_{T,B}}\delta z_P}\right)$$

Reinserting the result into the first equation, we have:

$$C_{TT}\frac{\partial T}{\partial t} + C_{T\Psi}\frac{\partial \Psi}{\partial t}$$
$$= K_{TT,E}T_E + K_{TT,W}T_W + K_{TT,N}T_N + K_{TT,S}T_S + K_{TT,T}T_T + K_{TT,B}T_B + K_{TT,P}T_P$$
$$+ K_{T\Psi,E}\Psi_E + K_{T\Psi,W}\Psi_W + K_{T\Psi,N}\Psi_N + K_{T\Psi,S}\Psi_S + K_{T\Psi,T}\Psi_T + K_{T\Psi,B}\Psi_B$$
$$+ K_{T\Psi,P}\Psi_P + \frac{\mathrm{g_{T,P}}}{\delta z_P}\left(\frac{\mathrm{g_{T,T}}(\delta z_P + \delta z_T)}{\mathrm{g_{T,P}}\delta z_T + \mathrm{g_{T,T}}\delta z_P} - \frac{\mathrm{g_{T,B}}(\delta z_P + \delta z_B)}{\mathrm{g_{T,P}}\delta z_B + \mathrm{g_{T,B}}\delta z_P}\right)$$

where

$K_{TT,E} = \frac{2k_{TT_P}k_{TT_E}}{\delta x_P\left(k_{TT_E}\delta x_P + k_{TT_P}\delta x_E\right)}$ and so on and $K_{TT,P} = -\left(K_{TT,E} + K_{TT,W} + K_{TT,N} + K_{TT,S} + K_{TT,T} + K_{TT,B}\right)$

Finally, using the same technique for both heat and mass equations, we obtain Equation (8).

$$\begin{aligned} C_{TT}\frac{\partial T}{\partial t} + C_{T\Psi}\frac{\partial \Psi}{\partial t} &= K_{TT}\mathrm{T} + K_{T\Psi}\Psi + \mathrm{G_T} + B_T \\ C_{\Psi T}\frac{\partial T}{\partial t} + C_{\Psi\Psi}\frac{\partial \Psi}{\partial t} &= K_{\Psi T}\mathrm{T} + K_{\Psi\Psi}\Psi + \mathrm{G_\Psi} + B_\Psi \end{aligned} \qquad (8)$$

where C_{TT}, $C_{T\Psi}, C_{\Psi T}$ and $C_{\Psi\Psi}$ are diagonal mass matrix, K_{TT}, $K_{T\Psi}$, $K_{\Psi T}$ and $K_{\Psi\Psi}$ are tridiagonal by bloc stiffness matrixes, $\mathrm{G_T}$ and $\mathrm{G_\Psi}$ are load vectors and B_T and B_Ψ are boundary

vectors. As all these matrixes depend on the variables T and Ψ, it's necessary to write an efficient programme able to compute it quickly for each iteration and time step.

4.2 Temporal discretization

Once the spatial derivatives have been removed from the continuous equation, we need to evaluate the temporal derivatives. This has been done using an implicit forward Euler method. An example for the heat equation is given in Equation (9), where Δt denotes the time step, eventually variable.

$$C_{TT}^{t+\Delta t}\left(T^{t+\Delta t}-T^{t}\right)+C_{T\Psi}^{t+\Delta t}\left(\Psi^{t+\Delta t}-\Psi^{\mathrm{t}}\right) = \Delta t K_{TT}^{t+\Delta t}\mathrm{T}^{t+\Delta t}+\Delta t K_{T\Psi}^{t+\Delta t}\Psi^{t+\Delta t}+\Delta t\left(G_{T}^{t+\Delta t}+B_{T}^{t+\Delta t}\right) \quad (9)$$

As the computational time is crucial for us, we chose to use a Newton-Raphson method to solve this matrix system. For each iteration, we have to solve $\Delta T^{t+\Delta t,m+1}$ as a solution of the Equation (10).

$$\frac{\partial \mathcal{L}}{\partial T}\left(T^{t+\Delta t,m}\right)\Delta T^{t+\Delta t,m+1}=-\mathcal{L}\left(T^{t+\Delta t,m}\right) \quad (10)$$

where

$$\mathcal{L}\left(T^{t+\Delta t}\right)=C_{TT}^{t+\Delta t}\left(T^{t+\Delta t}-T^{t}\right)+C_{T\Psi}^{t+\Delta t}\left(\Psi^{t+\Delta t}-\Psi^{\mathrm{t}}\right)-\Delta t K_{TT}^{t+\Delta t}\mathrm{T}^{t+\Delta t}-\Delta t K_{T\Psi}^{t+\Delta t}\Psi^{t+\Delta t} - \Delta t\left(G_{T}^{t+\Delta t}+B_{T}^{t+\Delta t}\right)=0$$

$$\frac{\partial \mathcal{L}}{\partial T}\left(T^{t+\Delta t,m}\right)=\frac{\partial (C_{TT}T)^{t+\Delta t,m}}{\partial T}+C_{TT}^{t+\Delta t,m}-\frac{\partial (C_{TT}T^{t})^{t+\Delta t,m}}{\partial T}+\frac{\partial \left(C_{T\Psi}\Psi^{t+\Delta t,m}\right)^{t+\Delta t,m}}{\partial T} - \frac{\partial (C_{T\Psi}\Psi^{t})^{t+\Delta t,m}}{\partial T}-\Delta t\frac{\partial (K_{TT}T)^{t+\Delta t,m}}{\partial T}-\Delta t K_{TT}^{t+\Delta t}-\Delta t\frac{\partial (K_{T\Psi}\Psi)^{t+\Delta t,m}}{\partial T} - \Delta t\frac{\partial (\mathrm{G_T}+B_{T})^{t+\Delta t,m}}{\partial T}$$

the jacobian matrix of the function $\mathcal{L}$.

Neglecting the term $\left(\frac{\partial \left(C_{TT}\Delta T^{t+\Delta t}\right)^{t+\Delta t,m}}{\partial T}+\frac{\partial \left(C_{T\Psi}\Delta\Psi^{t+\Delta t}\right)^{t+\Delta t,m}}{\partial T}\right)\boldsymbol{\Delta T^{t+\Delta t,m+1}}-C_{TT}^{t+\Delta t,m}\Delta T^{t+\Delta t}-C_{T\Psi}^{t+\Delta t,m}\Delta\Psi^{t+\Delta t}$, solve the Equation (10) is equivalent to solve

$$\left[C_{TT}^{t+\Delta t,m}-\Delta t K_{TT}^{t+\Delta t} - \Delta t\left(\frac{\partial (K_{TT}T)^{t+\Delta t,m}}{\partial T}+\frac{\partial (K_{T\Psi}\Psi)^{t+\Delta t,m}}{\partial T}+\frac{\partial (\mathrm{G_T}+B_{T})^{t+\Delta t,m}}{\partial T}\right)\right]\boldsymbol{\Delta T^{t+\Delta t,m+1}} = \Delta t\left(K_{TT}^{t+\Delta t,m}\mathrm{T}^{t+\Delta t,m}+K_{T\Psi}^{t+\Delta t,m}\Psi^{t+\Delta t,m}+G_{T}^{t+\Delta t,m}+B_{T}^{t+\Delta t,m}\right)$$

Where, calling $\mathcal{V}(i)$ the neighbourhood of the mesh number i, we have for example

$$\left(\frac{\partial (K_{TT}T)^{t+\Delta t,m}}{\partial T}\right)_{i,j} = \begin{cases} 0 \; if \; j \notin \mathcal{V}(i) \\ \left(T_j - T_i\right)\dfrac{\partial K_{TT}^{t+\Delta t,m}{}_{i,j}}{\partial T_j} if \; j \in \mathcal{V}(i) et \; j \neq i \\ \displaystyle\sum_{\substack{k\in\mathcal{V}(i)\\ k\neq i}} \frac{\partial K_{TT}^{t+\Delta t,m}{}_{i,k}}{\partial T_i} T_k^{t+\Delta t,m} - \left(\sum_{\substack{k\in\mathcal{V}(i)\\ k\neq i}} \frac{\partial K_{TT}^{t+\Delta t,m}{}_{i,k}}{\partial T_i}\right) T_i^{t+\Delta t,m} \; if \; i = j \end{cases}$$

where

$$\frac{\partial K_{TT}^{t+\Delta t,m}{}_{i,j}}{\partial T_j} = \frac{\delta x_j\left(\delta x_j + \delta x_i\right)\frac{\partial\left(k_{TT,j}^{t+\Delta t,m}\right)}{\partial T_j}\left(k_{TT,i}^{t+\Delta t,m}\right)^2}{\left(\delta x_i k_{TT,j}^{t+\Delta t,m} + \delta x_j k_{TT,i}^{t+\Delta t,m}\right)^2} \text{ and } \frac{\partial K_{TT}^{t+\Delta t,m}{}_{i,k}}{\partial T_i} = \frac{\delta x_i\left(\delta x_k + \delta x_i\right)\frac{\partial\left(k_{TT,i}^{t+\Delta t,m}\right)}{\partial T_i}\left(k_{TT,k}^{t+\Delta t,m}\right)^2}{\left(\delta x_i k_{TT,k}^{t+\Delta t,m} + \delta x_k k_{TT,i}^{t+\Delta t,m}\right)^2}$$

Using the same method for the heat and mass transfer equation, we can first solve the heat equation, and use the new temperature value $T^{t+\Delta t,m+1}$ into the mass equation, until convergence. This has been compared to a simultaneous resolution, which has been given up because it didn't decrease the number of iteration, and the computational time was higher (solve two n order equations is faster than solve one $2n$ order equation).

4.3 Boundary conditions

The boundaries conditions have been the most difficult part of this modelling work, especially the convective and the evaporation / condensation terms.

a. On the ground surface, the heat and mass equation to solve are:

$$-k_{TT}\nabla \mathrm{T}|_{\mathrm{z=H}} - k_{T\Psi}\nabla\Psi|_{\mathrm{z=H}} + \mathrm{h_c}(\mathrm{T_a} - \mathrm{T_S}) + \left(1 - \alpha_\mathrm{d}\left(1 - \frac{\theta_\mathrm{S}}{2\theta_\mathrm{s}}\right)\right)\mathrm{R} + \sigma\varepsilon\left(\mathrm{T_{sky}^4} - \mathrm{T_S^4}\right)$$
$$+ \left(\mathrm{L_0} + \mathrm{c_v}(\mathrm{T_S} - \mathrm{T_0})\right)\mathrm{D_v}\left(\rho_{\mathrm{v,a}} - \rho_{\mathrm{v,S}}\right) + \mathrm{C_l}(\mathrm{T_a} - \mathrm{T_0})\mathrm{P} = 0$$

$$-\rho_l(k_{\Psi\Psi}\nabla\Psi|_{\mathrm{z=H}} + k_{\Psi\mathrm{T}}\nabla \mathrm{T}|_{\mathrm{z=H}} + K_h) + P + \mathrm{D_v}\left(\rho_{\mathrm{v,a}} - \rho_{\mathrm{v,S}}\right) = 0$$

with

$$\mathrm{h_c} = \left(\mathrm{h_f^4} + \mathrm{h_n^4}\right)^{1/4}$$

where

$$h_f = \rho_\mathrm{a} C_\mathrm{a} \mathrm{D_h}$$

$$h_n = 0.15\lambda_\mathrm{a}\left(\frac{g(T_s - T_a)}{T_f \nu_\mathrm{a}\alpha_\mathrm{a}}\right)^{1/3}$$

$$R_i = \frac{g(\mathrm{T_a} - \mathrm{T_S})(z_e - z_0)}{\mathrm{T_a}V^2}$$

$$D_h = \begin{cases} \dfrac{\kappa^2 V}{ln\left(\frac{z_e}{z_0}\right)^2}(1-5R_i)^{0.75} si\ R_i \le 0 \\ 0 \text{ si } R_i > 0.2\ et\ si\ R_i < -5 \\ \dfrac{\kappa^2 V}{ln\left(\frac{z_e}{z_0}\right)^2}(1-5R_i)^2 si\ 0 < R_i \le 0.2 \end{cases}$$

$$D_v = \left(\max(810 - 4140\theta_S, 0) + \frac{1}{\frac{h_c}{\rho_a C_a}\left(\frac{D_{va}}{\alpha_a}\right)^{2/3}} \right)^{-1}$$

b. On the base layer, the equations are:

$$-k_{TT}\nabla T|_{z=0} - k_{T\Psi}\nabla\Psi|_{z=0} + c_l\rho_l(T_B - T_0)K_h(1 - \nabla\Psi|_{z=0}) + \rho_l\left(L_0 + (c_v - c_l)(T_B - T_0)\right)\left(D_{Tv}\nabla T|_{z=0} + D_{\Psi v}\nabla\Psi|_{z=0}\right) = 0$$

$$\Psi_B = 0$$

as the bottom of the ground element is assumed to reach the water table.

c. On the cavity of the foundation:

$$-k_{TT}\nabla T|_{edge} - k_{T\Psi}\nabla\Psi|_S + h_c(T_{a,j} - T_S) + \frac{(L_0 + c_v(T_S - T_0))}{C_a} h_{conv}\left(\frac{\rho_{va,j}}{\rho_{aij}} - \frac{\rho_{vS}}{\rho_{aS}}\right) = 0$$

$$-\rho_l(K_h\nabla\Phi|_S + k_{\Psi\Psi}\nabla\Psi S + k_{\Psi T}\nabla T|_S) + \frac{h_c}{C_a}\left(\frac{\rho_{va,j}}{\rho_{a,j}} - \frac{\rho_{vS}}{\rho_{sS}}\right) = 0$$

with the terms $\left(\frac{\rho_{va,j}}{\rho_{aij}} - \frac{\rho_{vS}}{\rho_{aS}}\right)$ constraint by what has been said in 3.3.

The Newton-Raphson method is once again adopted to compute the values of T and Ψ on the surfaces.

5 Results

As we encountered a lot of numerical problems, most of them being a consequence of the boundary equation encoding, we only achieved to model a 1m X 15cm x 4.5m ground element exposed to real climatic conditions at surface got from the monitoring in the framework of FONDATHERM, and adiabatic condition on all other faces. The Figure 7 shows the atmospheric excitation imposed at ground surface. The Figure 8 shows the results got from the simulation on one day with a 10min time step.

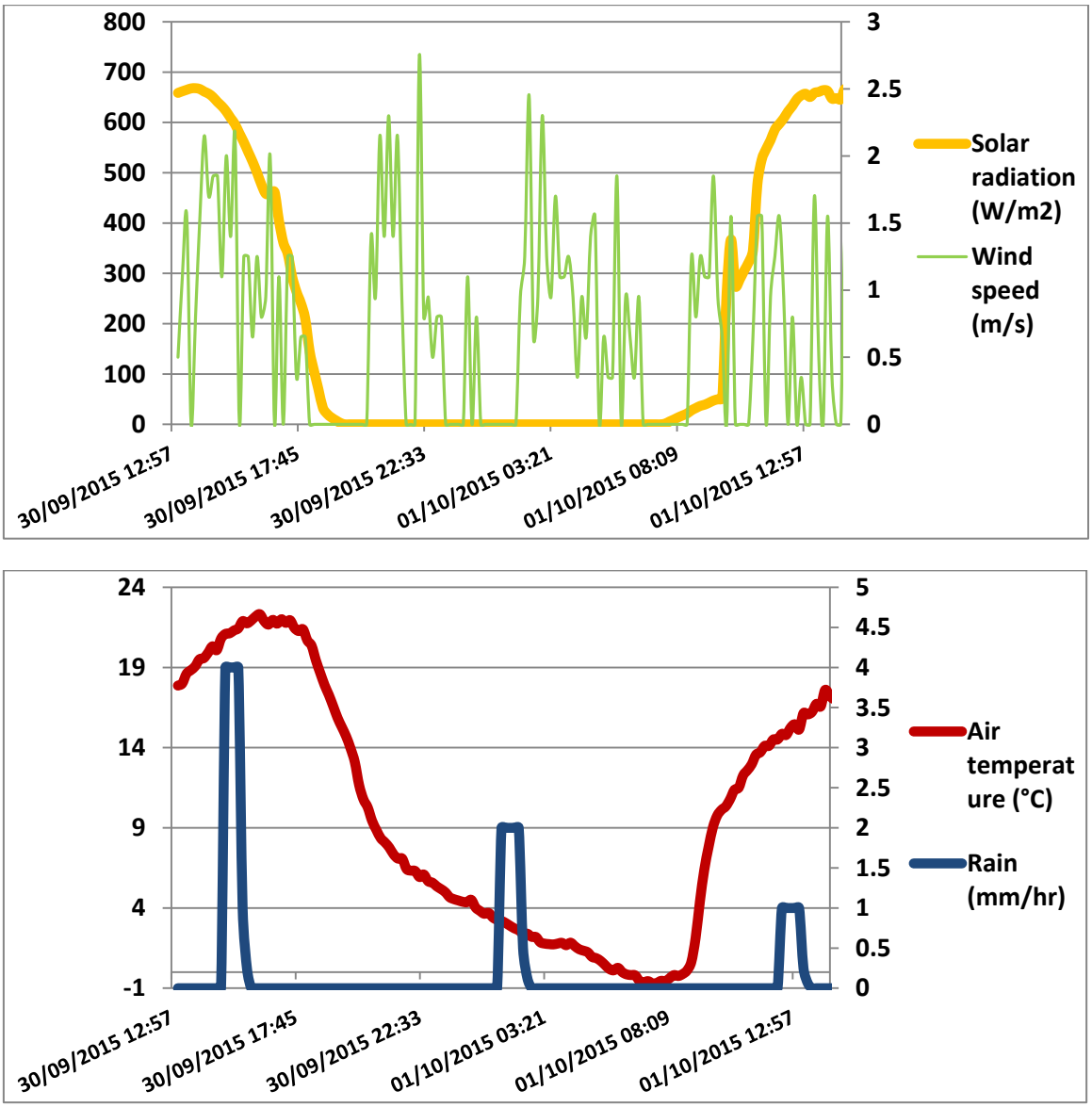

Figure 7 : Atmospheric excitation : Solar radiation, wind speed, aire temperature and rain

The rain has been artificially added to the weather data to evaluate the behaviour of the model close to water saturation.

20h12

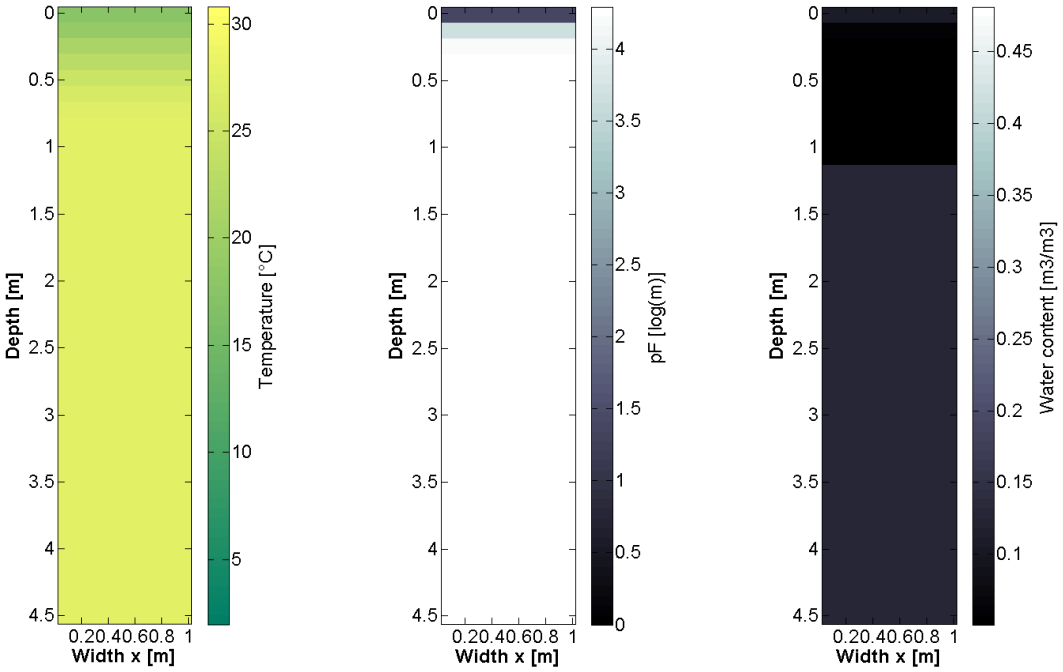

Figure 8 : Temperature (°C), matric head (log(m)), and moisture content (m3/m3) of a ground cross section

00h42

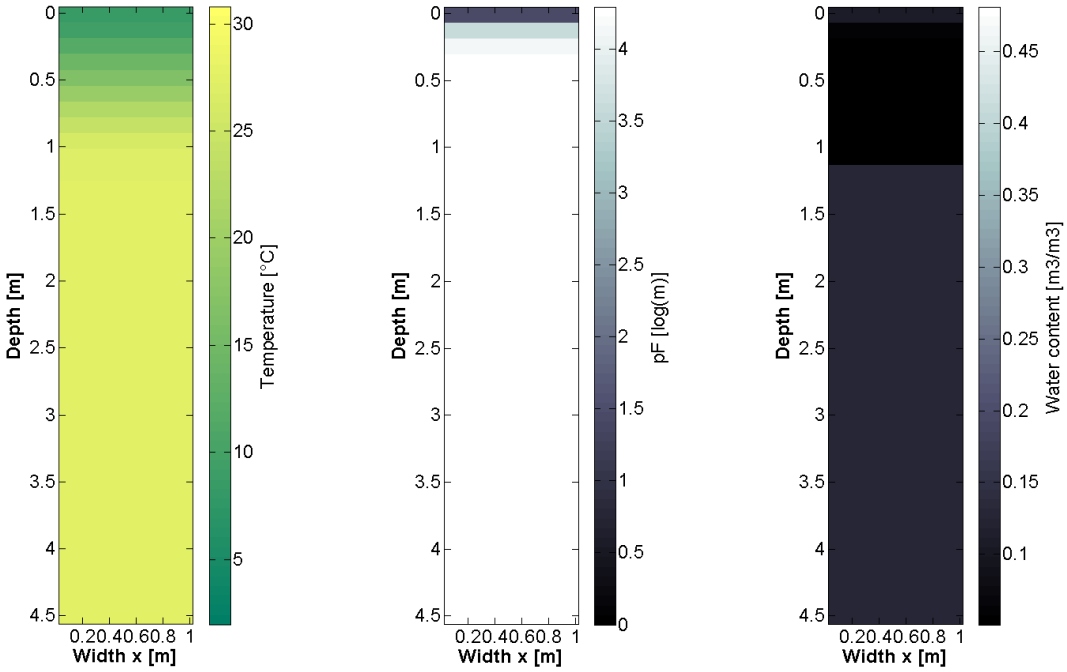

05h42

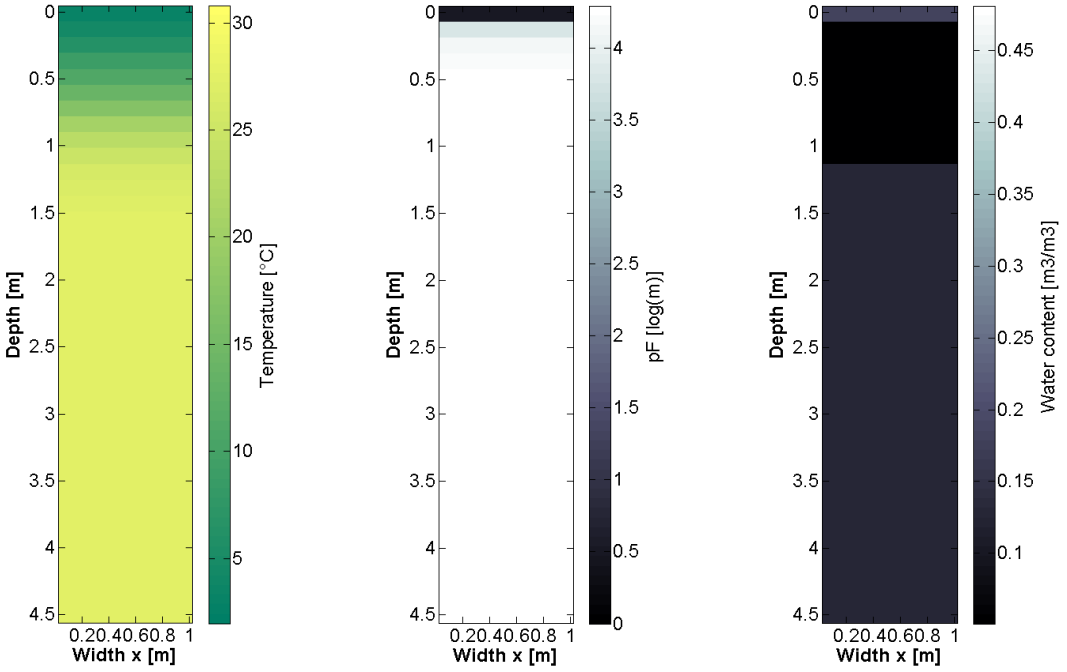

Figure 9 : Temperature (°C), matric head (log(m)), and moisture content (m3/m3) of a ground cross section

11h42

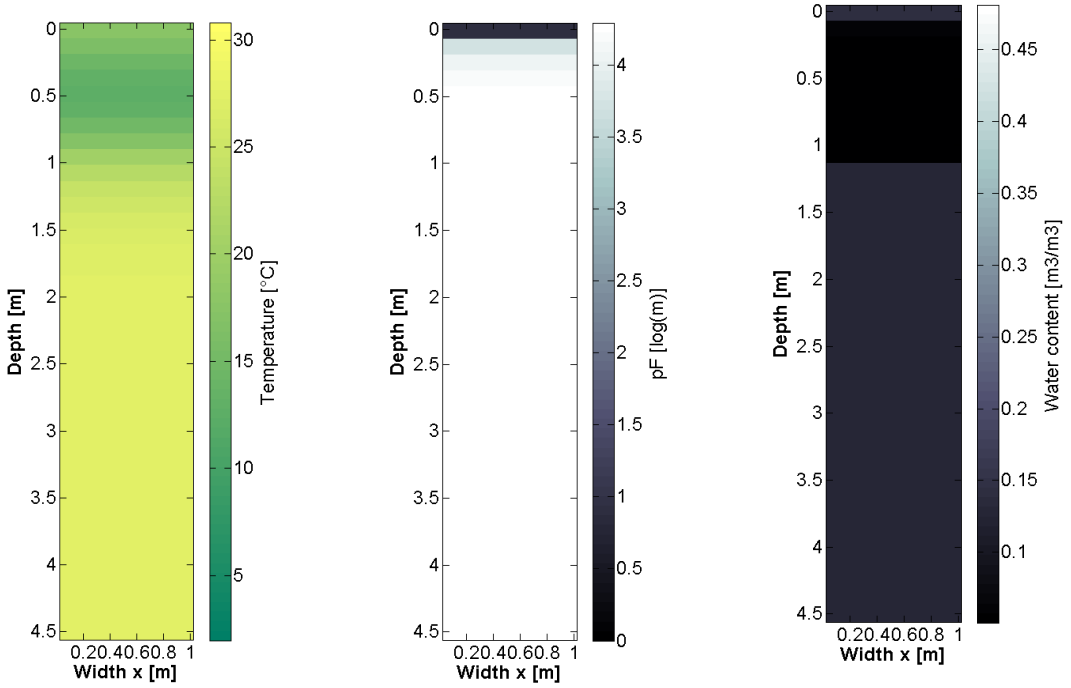

14h42

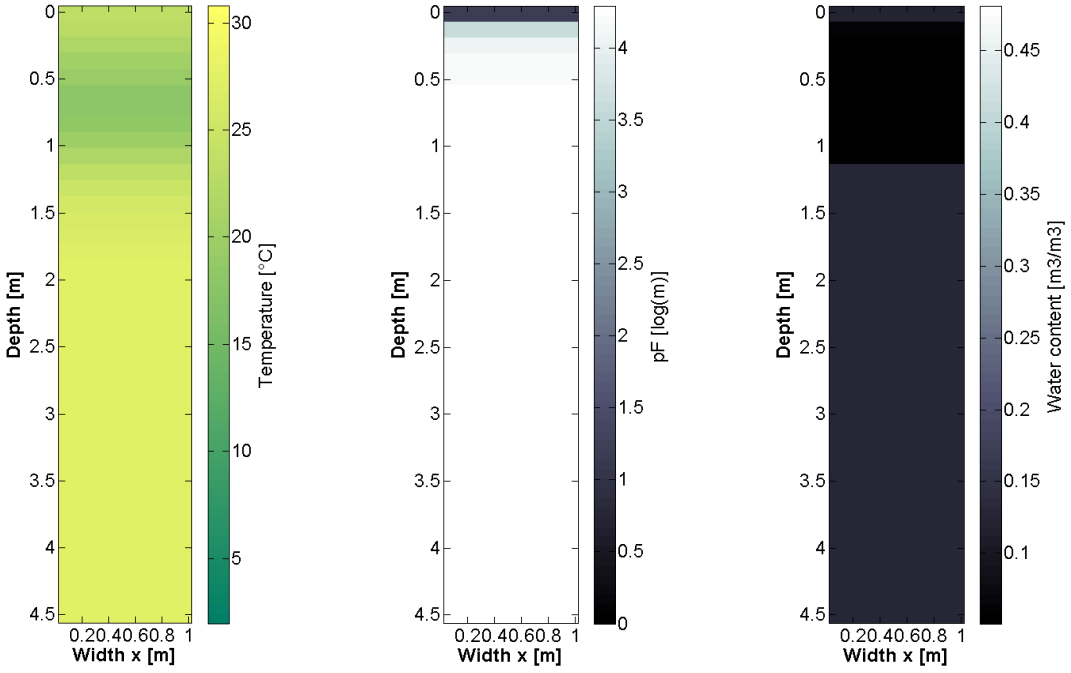

Figure 10 : Temperature (°C), matric head (log(m)), and moisture content (m3/m3) of a ground cross section

As we can observe, the behaviour of the model seems relevant. The thermal outdoor wave propagates well within the ground. The matric head graphs show that the moisture is drained from the top to the bottom of the ground after the rains. The discontinuity in the water content profile is explained by the fact that two materials have been used to construct the ground element: sand for the first metre, and clay for the base layer. We can also observe that the temperature of the ground is really high. This is due to the fact that the initialisation was for a sunny and hot time step. It shows the importance to run the code for several months in order to eliminate the influence of the initial conditions.

There remain still some difficulties currently under investigation. These include:

- Problem of convergence during rainfall events. This could be solved using the variable time step method used by [13]
- Problem of convergence when the wind velocity is low. The convection model has been changed to include natural convection, which improved the convergence
- Problem of convergence when the boundary condition “water table” is added at the bottom. During the iterative process to solve the system of equation at the first time step, this boundary leads to very high (positive) matric head. This could be solved by adding a condition in the Matlab code, according to Janssen

6 Outcomes or future work

First the ground model has to be validated against data available on literature, for which analytic solution exist. Then, the foundation will be added, and the whole model will be compared to the experimental data got from the facilities in the framework of FONDATHERM. Once validated, the PCM layer will be added onto the cavity. Several simulations, testing different melting point at different places along the foundation will be carried on. Finally, in order to lead accurate simulation on several years with fine meshing, we would like to reduce the equation using a Proper Generalized Decomposition (PGD) method, as used for the same kind of physical problem in [29].

7 References

[1] Mihalakakou, G., Santamouris, M., Asimakopoulos, D. « Modelling the thermal performance of earth-to-air heat exchangers ». *Solar Energy* 53 (1994b.), 301-305.

[2] Carol Gauthier, Marcel Lacroix, Hervé Bernier. « Numerical simulation of soil heat exchanger-storage systems for greenhouses". *Solar Energy* 60, Issue 6, (1997): 333-346.

[3] Hollmuller, P. (2002). Utilisation des échangeurs air/sol pour le chauffage et le rafraîchissement des bâtiments : Mesures in situ, modélisation analytique, simulation numérique et analyse systémique.

[4] Thiers, Stéphane, Bruno Peuportier. « Thermal and Environmental Assessment of a Passive Building Equipped with an Earth-to-Air Heat Exchanger in France ». *Solar Energy* 82, no 9 (2008): 820-31.

[5] Tittelein, Pierre, Gilbert Achard, Etienne Wurtz. « Modelling Earth-to-Air Heat Exchanger Behaviour with the Convolutive Response Factors Method ». *Applied Energy* 86, no 9 (2009).

[6] Trząski, Adrian, Bernard Zawada. « The Influence of Environmental and Geometrical Factors on Air-Ground Tube Heat Exchanger Energy Efficiency ». *Building and Environment* 46, no 7 (2011): 1436-44.

[7] Su, Hua, Xiao-Bing Liu, Lei Ji, Jing-Yu Mu. « A Numerical Model of a Deeply Buried Air–earth–tunnel Heat Exchanger ». *Energy and Buildings* 48 (2012): 233-39.

[8] Vaz, Joaquim, Miguel A. Sattler, Elizaldo D. dos Santos, Liércio A. Isoldi. « Experimental ans Numerical Analysis of an Earth-Air Heat Exchangers ». *Energy and Buildings* 43 (2011): 2476-82.

[9] Bansal, Vikas, Rohit Misra, Ghanshyam Das Agarwal, Jyotirmay Mathur. « Transient Effect of Soil Thermal Conductivity and Duration of Operation on Performance of Earth Air Tunnel Heat Exchanger ». Applied Energy 103 (2013): 1-11.

[10] Gan, Guohui. « Simulation of Dynamic interactions of the Earth-Air Heat Exchanger with Soil and atmosphere for Preheating of Ventilation Air ». *Applied energy* 158, (2015): 118-132.

[11] Deru, Michael P., Allan T. Kirkpatrick. « Ground-Coupled Heat and Moisture Transfer from Buildings Part 1–Analysis and Modeling* ». Journal of solar energy engineering 124, no 1 (2002): 10-16.

[12]Deru, Michael P. A model for ground-coupled heat and moisture transfer from buildings. National Renewable Energy Laboratory, (2003).

[13] Janssen, H. The influence of soil moisture transfer on building heat loss via the ground. *The Catholic University of Leuven* (2002).

[14] dos Santos, Gerson H., Nathan Mendes. « Simultaneous Heat and Moisture Transfer in Soils Combined with Building Simulation ». *Energy and Buildings* 38, no 4 (2006): 303-14.

[15] Kuznik, Frédéric, Joseph Virgone, Jean-Jacques Roux. « Energetic Efficiency of Room Wall Containing PCM Wallboard: A Full-Scale Experimental Investigation ». *Energy and Buildings* 40, n° 2 (2008): 148-56.

[16] Hichem, Necib, Settou Noureddine, Saifi Nadia, Damene Djamila. « Experimental and Numerical Study of a Usual Brick Filled with PCM to Improve the Thermal Inertia of Buildings ». *Energy Procedia* 36 (2013): 766-75.

[17] Rouault, Fabien, Denis Bruneau, Patrick Sébastian, Jérôme Lopez. « Experimental Investigation and Modelling of a Low Temperature PCM Thermal Energy Exchange and Storage System ». *Energy and Buildings* 83 (2014): 96-107.

[18] de Gracia, Alvaro, Lidia Navarro, Albert Castell, Luisa F. Cabeza. « Numerical Study on the Thermal Performance of a Ventilated Facade with PCM ». *Applied Thermal Engineering* 61, n° 2 (2013): 372-80.

[19] Jaworski, Maciej, Piotr Łapka, Piotr Furmański. « Numerical Modelling and Experimental Studies of Thermal Behaviour of Building Integrated Thermal Energy Storage Unit in a Form of a Ceiling Panel ». *Applied Energy* 113 (2014): 548-57.

[20] Rodrigues, Lucelia Taranto, Mark Gillott. « A Novel Low-Carbon Space Conditioning System Incorporating Phase-Change Materials and Earth–air Heat Exchangers ». *International Journal of Low-Carbon Technologies* 10, no 3 (2015): 176-87.

[21] Philip, J. R., et D. A. De Vries. « Moisture movement in porous materials under temperature gradients ». *Eos, Transactions American Geophysical Union* 38, no 2 (1957): 222-32.

[22] D. A. De Vries. « Simultaneous transfer of heat and moisture in porous media ». *Eos, Transactions American Geophysical Union* 39, no 5 (1958): 909-16.

[23] De Vries, D.A. « Thermal properties of soils ». *Physics of plant environment,* (W.R. Van Wok, Ed.). Amsterdam: North-Holland Publishing Company.

[24] Zhang, H.-F., X.-S. Ge, H. Ye, D.-S. Jiao. « Heat Conduction and Heat Storage Characteristics of Soils ». *Applied Thermal Engineering* 27, no 2-3 (2007): 369-73.

[25] Van Genuchten M. Th. « A closed-form equation for predicting the hydraulic conductivity of unsaturated soils ». *Soil Science Society of America Journal* 44, no 5 (1980): 892-98.

[26] Vogel T., van Genuchten M. Th., Cislerova M. « Effect of the shape of the soil hydraulic functions near saturation on variably-saturated flow predictions ». *Advances in Water Resources* 24, (2001): 133-44.

[27] Mualem Y., « A conceptual model of hysteresis ». *Water resources research* 10, no 3 (1974): 514-20.

[28] van Genuchten M. Th., Nielsen D. R., « On describing and predicting the hydraulic properties of unsaturated soils ». *Annales Geophysicae 3,* no5 (1985): 615-28.

[29] Mualem Y., « A new model for predicting the hydraulic conductivity of unsaturated porous media ». *Water resources research* 12, no 3 (1976): 513-22.

[30] Julien Berger. Contribution à la modélisation hygrothermique des bâtiments : application des méthodes de réduction de modèle. Civil Engineering. Université de Grenoble, 2014. French.

[31] Labat, Matthieu. Chaleur-Humidité-Air dans les maisons à ossature bois: expérimentation et modélisation. INSA de Lyon, 2012.

[32] Janssen H., Blocken B., Carmeliet J., « Conservative modeling of the moisture and heat transfer in building components under atmospheric excitation ». *International Journal of Heat and Mass Transfer* 50, (2007): 1128-40.

[33] Soares, N., J.J. Costa, A.R. Gaspar, P. Santos. « Review of Passive PCM Latent Heat Thermal Energy Storage Systems towards Buildings' Energy Efficiency ». *Energy and Buildings* 59 (2013): 82-103.

[34] Lamberg, Piia, Reijo Lehtiniemi, Anna-Maria Henell. « Numerical and Experimental Investigation of Melting and Freezing Processes in Phase Change Material Storage ». *International Journal of Thermal Sciences* 43, n° 3 (2004): 277-87.

[35] Al-Saadi, Saleh Nasser, Zhiqiang (John) Zhai. « Systematic Evaluation of Mathematical Methods and Numerical Schemes for Modeling PCM-Enhanced Building Enclosure ». *Energy and Buildings* 92 (2015): 374-88.

[36] Tittelein, Pierre, Stéphane Gibout, Erwin Franquet, Kevyn Johannes, Laurent Zalewski, Frédéric Kuznik, Jean-Pierre Dumas, Stéphane Lassue, Jean-Pierre Bédécarrats, Damien David. « Simulation of the Thermal and Energy Behaviour of a Composite Material Containing Encapsulated-PCM: Influence of the Thermodynamical Modelling ». *Applied Energy* 140 (2015): 269-74.

[37] Patankar S. V., « Numerical heat transfer and fluid flow». *Series in computational methods in mechanics and thermal sciences.* 1980: 197 pages.

8 Assessment

Give your personal opinion about the secondment